

High-Mobility and High-Reliability Top-Gate Oxide Semiconductor Transistors by Oxygen Engineering

Kai Jiang, Zhiyu Lin, Ziheng Wang, Chen Wang, Mengwei Si

Abstract—In this work, we investigate the role of oxygen (O) on the performance of top-gate (TG) atomic-layer-deposited (ALD) oxide semiconductor transistors. The results reveal distinct defect characteristics and positive bias temperature instability (PBTI) degradation mechanisms between oxygen-rich (O-rich) and oxygen-deficient (O-poor) devices. It is found that an O-rich device fabrication process followed by O-free annealing can effectively achieve TG indium-rich (In-rich) oxide semiconductor transistors with high mobility, high reliability and high stability in hydrogen environment because O-rich process can suppress oxygen vacancies and their interaction with hydrogen, while O-free annealing plays a critical role in minimizing the formation of O-rich defects such as oxygen dimers (O-O bonds). Consequently, TG In-rich transistors with high mobility, steep subthreshold slope, and high PBTI reliability at high temperature are demonstrated. The understanding of O-rich defects provides a new insight to overcome the mobility-stability trade-off.

Index Terms—oxide semiconductor, high mobility, high reliability, defects.

I. INTRODUCTION

Oxide semiconductor (OS) transistors are considered as promising candidates as back-end-of-line (BEOL) compatible devices for monolithic 3D integration and dynamic random-access memory (DRAM) applications [1-7]. Recent advances in bottom-gate (BG) OS transistors have demonstrated significant improvements in device performance and reliability [8-15]. However, the mechanism for threshold voltage shift (ΔV_{TH}) in the positive bias temperature instability (PBTI) test is still not clear. Meanwhile, high-mobility OS have deeper conduction-band minimum (CBM) and smaller activation energy, which implies that they have lower tolerance to defects, leading to the mobility-stability trade-off [16]. To date, several studies have proposed possible defects for donor in OS, such as oxygen vacancies (V_O), hydrogen (H), and the interaction between V_O and H [17-23], but there is still no

Manuscript received xxx xx, xxxx. This work was supported by the National Key Research and Development Program of China under Grant 2022YFB3606900, National Natural Science Foundation of China under Grant 62274107, 92264204 and Shanghai Pilot Program for Basic Research-Shanghai Jiao Tong University under Grant 21TQ1400212. (Corresponding author: Mengwei Si.)

Kai Jiang, Zhiyu Lin, Ziheng Wang, Chen Wang, Mengwei Si are with State Key Laboratory of Micro and Nano Engineering Science and the School of Information Science and Electronic Engineering, Shanghai Jiao Tong University, Shanghai 200240, China (email: mengwei.si@sjtu.edu.cn).

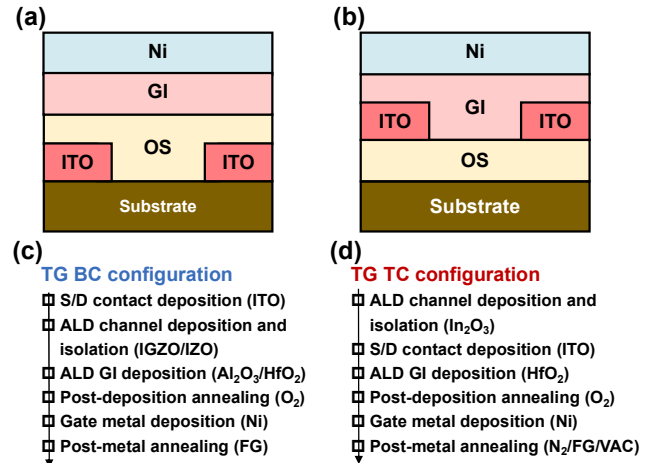


Fig. 1 (a) Schematic diagram of TG (a) BC and (b) TC OS transistors. The device fabrication process flow of (c) TG BC and (d) TG TC devices.

consensus on the exact nature of the defects involved or their specific impact on reliability. In fact, ΔV_{TH} during PBTI test arises from interplay of various defects and similar ΔV_{TH} trends may originate from distinct physical process, making it difficult to investigate the intrinsic mechanism.

Compared with BG OS transistors, top-gate (TG) OS transistors are more preferred due to their superior integration density and lower parasitic capacitance. For TG structure, the main challenge lies in the generation of V_O during atomic layer deposition (ALD) of gate insulator (GI) on OS channels, caused by metal precursor-induced oxygen scavenging [24-36]. Such an effect is particularly severe for high-mobility indium-rich (In-rich) OS, as In-O bonds exhibit relatively low stability during the GI deposition process [37], [38]. And the interaction between V_O and H results in performance degradation and poor PBTI reliability and stability in H environment. Therefore, although TG OS transistors with relatively low-mobility channels have been reported with high reliability [39-44], the reliability characteristics of TG high-mobility In-rich OS devices remain insufficiently investigated.

In this work, the distinct difference in defect characteristics and PBTI degradation mechanisms between oxygen-rich (O-rich) and oxygen-deficient (O-poor) devices is revealed. It is found both O-rich and O-poor defects lead to similar negative V_{TH} shift during device fabrication, so that confusing results and explanation are commonly reported in literature. We propose and verify that an O-rich device fabrication process followed by oxygen-free (O-free) annealing can simultaneously suppress both O-poor and O-rich defects to achieve high-

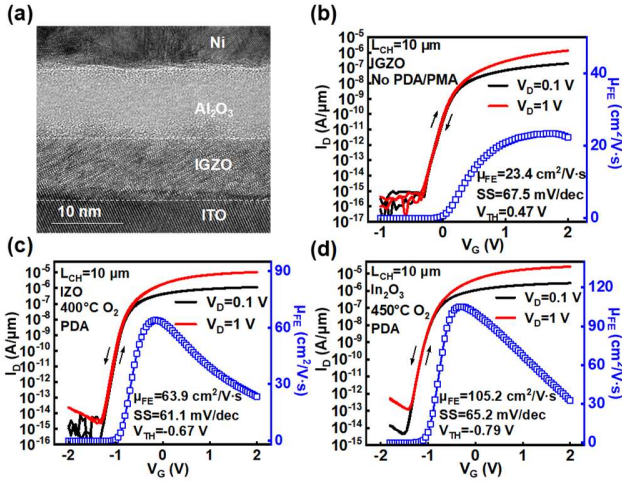


Fig. 2 (a) The cross-sectional TEM image of the S/D region in a TG BC IGZO transistor. I_D - V_G and μ_{FE} - V_G characteristics of TG (b) IGZO, (c) IZO, and (d) In_2O_3 transistors with L_{CH} of 10 μm . TG In-rich devices show high performance since O_2 PDA effectively suppresses the concentration of V_O .

mobility TG In-rich OS transistors with enhanced reliability and stability in H environment. The O-rich fabrication process is essential for suppressing V_O and their interaction with H, while the O-free annealing is critical for minimizing the formation of O-rich defects. As a result, we demonstrate TG ALD In_2O_3 transistors with high field-effect mobility (μ_{FE}), steep subthreshold slope (SS) and high PBTI reliability at high temperature. The understanding of O-rich defects can provide a new insight to overcome the mobility-stability trade-off.

II. EXPERIMENTS

Figs. 1(a) and 1(b) exhibit the schematic diagram of the TG OS transistors with bottom-contact (BC) and top-contact (TC) configurations. The corresponding device fabrication process flow is shown in Figs. 1(c) and 1(d). For BC configuration, source/drain (S/D) electrodes are deposited before channel deposition while S/D electrodes deposition after channel deposition for TC configuration. The device fabrication started with a Si substrate with 90 nm thermally grown SiO_2 and 10 nm ALD Al_2O_3 as buffer layer. For the BC structure, 80 nm ITO was deposited by sputtering on substrate as S/D electrodes. Then 10 nm IGZO or 8 nm IZO was deposited as OS channel. Channel isolation was achieved through wet etching with hydrochloric acid (HCl). For the TC structure, 4 nm In_2O_3 was deposited by ALD as OS channel, followed by channel isolation. Subsequently, 80 nm ITO was deposited by sputtering as S/D electrodes. 10 nm ALD Al_2O_3 using trimethylaluminum (TMA) and H_2O as precursors for IGZO channel or 8 nm ALD HfO_2 with tetrakis(dimethylamido)hafnium (TDMAHf) and O_3 as precursors for IZO and In_2O_3 channels was deposited as GI. The growth temperature of both HfO_2 and Al_2O_3 is 200°C. PDA was conducted in O_2 at various temperatures for 10 min. 40 nm Ni was deposited by thermal evaporation as gate metal. Finally, PMA was performed in N_2 or vacuum (VAC) or forming gas (FG, 4% $H_2/96\% N_2$) at various temperatures for 10 min. The cross-sectional transmission electron microscopy (TEM) image in a typical TG BC IGZO transistor is shown in Fig. 2(a).

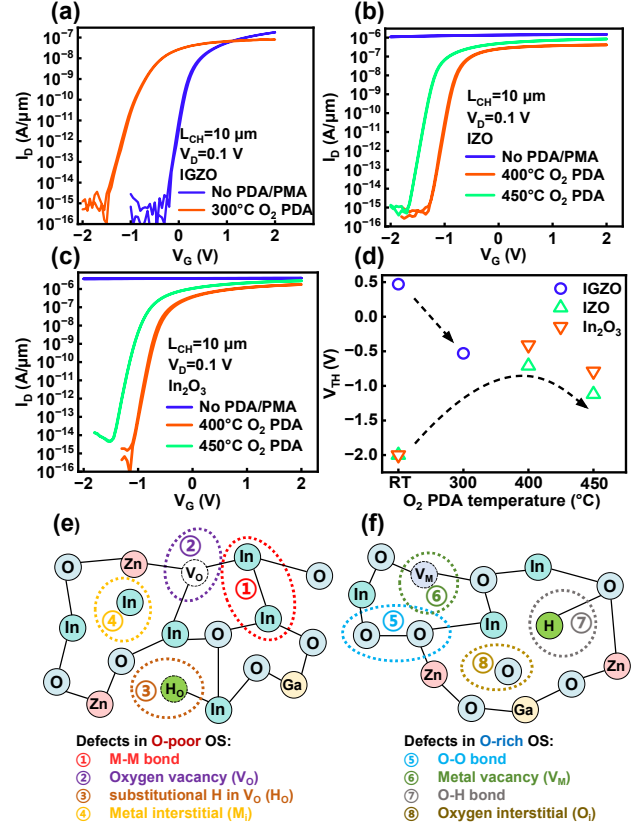


Fig. 3 Transfer characteristics of TG (a) IGZO, (b) IZO, and (c) In_2O_3 transistors under different annealing conditions. (d) V_{TH} versus O_2 PDA temperature extracted from Figs. 3(a) to 3(c). IZO and In_2O_3 devices without annealing cannot be turned off and V_{TH} of -2 V is used here for comparison. The possible defect types in (e) O-poor and (f) O-rich OS films. The dominant defect types differ fundamentally between O-rich and O-poor films.

III. RESULTS AND DISCUSSION

Figs. 2(b) to 2(d) exhibit the I_D/μ_{FE} - V_G curves of TG OS transistors with channel length (L_{CH}) of 10 μm and different channel materials. TG IGZO transistors without annealing exhibit large on/off ratio. Moreover, although H_2O was used as precursor for Al_2O_3 GI, the devices without annealing still exhibit decent SS and on/off ratio. This result indicates only minimal degradation of the IGZO channel during GI deposition, which can be partly explained by the presence of Ga enhances the stability of IGZO, but the role of H here is not clear. In contrast, TG In-rich IZO and In_2O_3 devices without annealing cannot be turned off, indicating oxide atoms are taken away from the oxide channel layer due to oxygen scavenging by Hf precursors, resulting in damage to OS channel layer. High-temperature O_2 annealing can effectively suppress the concentration of V_O and the TG In-rich devices achieve high μ_{FE} , steep SS, and negligible hysteresis.

Oxygen PDA exerts a profound influence on device performance. Systematic annealing under varying conditions was therefore conducted to investigate the underlying mechanisms. Figs. 3(a) to 3(c) exhibit the transfer characteristics of TG OS transistors with different OS channels under different annealing conditions. For the TG IGZO

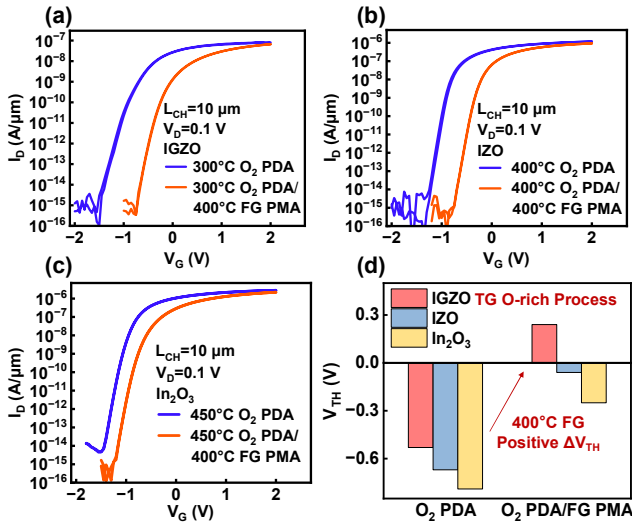


Fig. 4 Transfer characteristics of TG (a) IGZO, (b) IZO, and (c) In₂O₃ devices under different annealing conditions. (d) The impact of FG PMA on V_{TH} of TG O-rich devices extracted from Figs. 4(a) to 4(c). All devices exhibit more positive V_{TH} after additional FG PMA.

transistor, O₂ PDA induces a substantial negative ΔV_{TH} and degradation of SS. For both IZO and In₂O₃ channels, devices without annealing cannot be turned off, originating from V_O generation during GI deposition, where Hf precursors scavenge oxygen from OS channel layer, as previously reported [24], [37], [38]. With 400°C O₂ PDA, the devices exhibit a significant more positive V_{TH} , which is attributed to the effective suppression of V_O. However, as the O₂ PDA temperature rises to 450°C, an abnormal negative ΔV_{TH} is also observed, indicating the presence of donor-type O-rich defects, with their generation mechanism attributed to high-temperature O₂ annealing. Fig. 3(d) illustrates V_{TH} of the devices with different OS channels as a function of O₂ PDA temperature, clearly demonstrating an initial positive ΔV_{TH} followed by a negative ΔV_{TH} with increasing O₂ PDA temperature for both TG IZO and In₂O₃ transistors, indicating a transition from O-poor to O-rich state in the OS channels. For the IGZO channel, the device without annealing is not in O-poor state since the presence of Ga enhances the stability of IGZO, while 300°C O₂ PDA introduces excess O-rich defects, resulting in a negative ΔV_{TH} .

Based on the above experimental results, the possible defect types in the OS films are summarized in Figs. 3(e) and 3(f). The dominant defect types differ fundamentally between O-rich and O-poor films. Defects such as O-O bond, metal vacancy (V_M), O-H bond, metal interstitial (M_i), etc. may exist in O-rich film, while defects such as M-M bond, V_O, M-H bond (substitutional H in V_O, H_O), oxygen interstitial (O_i), etc. may exist in O-poor film. However, O-rich and O-poor devices may behave similarly even though the distinct defects exist in the OS films. It has been understood that H could react with V_O (O-poor defects), leading to negative ΔV_{TH} [19-22], [37]. High-temperature O₂ annealing could suppress O-poor defects while inducing O-rich defects, which also results in negative ΔV_{TH} through distinct mechanisms. Therefore, both O-poor and O-rich defects can exhibit donor-like behavior in the OS films, making it difficult to distinguish them.

To verify that the TG OS transistors with O₂ PDA are in O-rich state and O-rich defects can exhibit donor-like behavior,

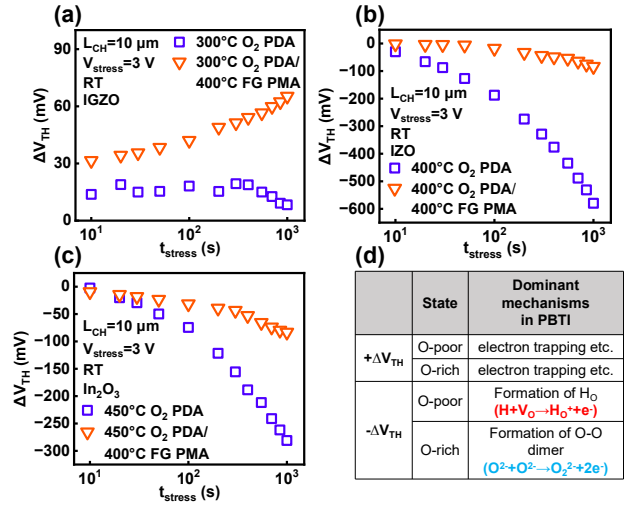


Fig. 5 ΔV_{TH} versus t_{stress} characteristics at RT of TG (a) IGZO, (b) IZO, and (c) In₂O₃ transistors under different annealing conditions. (d) Summary of PBTI degradation mechanisms in OS transistors and the dominant negative ΔV_{TH} mechanisms differ significantly between O-rich and O-poor devices owing to different defect types.

devices with O₂ PDA were annealed in FG. It has been understood that H could react with V_O (O-poor defects) leading to negative ΔV_{TH} and devices typically show negative ΔV_{TH} after FG annealing. Figs. 4(a) to 4(c) present the transfer characteristics of TG OS transistors with FG PMA after O₂ PDA. All devices exhibit more positive V_{TH} after additional FG PMA, indicating the interaction between H and V_O has been effectively suppressed since the concentration of V_O is reduced by O₂ PDA and the dominant defects in the device are not O-poor defects. Therefore, by O-rich fabrication process, stability in H environment at high temperature can be improved significantly without V_{TH} degradation. Fig. 4(d) summarizes the impact of FG PMA on V_{TH} of TG O-rich devices. The O-rich devices with O₂ PDA exhibit more positive V_{TH} after additional FG PMA, indicating that the O-rich defects are donor-like defects and the positive ΔV_{TH} after FG PMA suggests O-rich defects could be suppressed by O-free annealing.

More positive V_{TH} in the transfer characteristics after FG PMA indicates the devices with O₂ PDA are in O-rich state. To further confirm the generation of O-rich defects after high-temperature O₂ annealing, PBTI performance was measured. Figs. 5(a) to 5(c) show the PBTI performance of TG OS transistors with different annealing conditions at room temperature (RT). For IZO and In₂O₃ channels, devices with only O₂ PDA exhibit significant negative ΔV_{TH} . The negative ΔV_{TH} during PBTI is typically attributed to the interaction between H and V_O. However, the devices show high stability in H environment owing to the suppression of V_O by O₂ PDA and the negative ΔV_{TH} here should originate from other mechanisms. Moreover, ΔV_{TH} becomes more positive with additional FG PMA and the absolute value of ΔV_{TH} reduces significantly, confirming that the negative ΔV_{TH} observed in devices with only O₂ PDA does not originate from the interaction between V_O and H. FG PMA after O₂ PDA leads to more positive V_{TH} in the transfer characteristics and enhanced PBTI reliability. The enhancement of PBTI reliability by FG PMA provides compelling evidence that the negative ΔV_{TH} during PBTI test in devices with O₂ PDA originates from O-

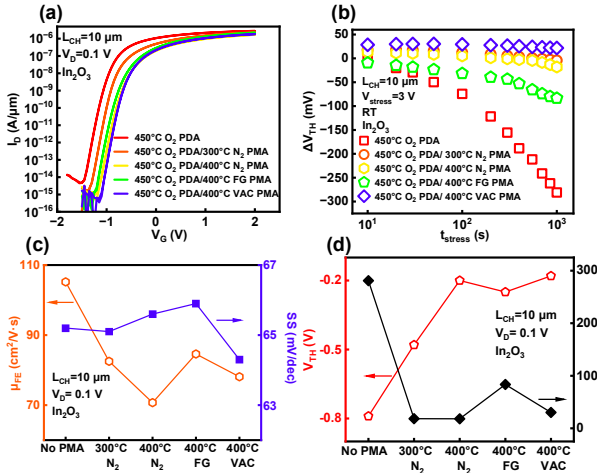


Fig. 6 (a) Transfer characteristics of TG In_2O_3 transistors with L_{CH} of 10 μm under different PMA conditions. (b) ΔV_{TH} versus t_{stress} characteristics at RT of TG In_2O_3 transistors with L_{CH} of 10 μm under different annealing conditions. (c) μ_{FE} and SS, (d) V_{TH} and $|\Delta V_{\text{TH}}|$ under PBTI at $V_{\text{stress}}=3$ V for 1 ks of TG In_2O_3 transistors with O_2 PDA and different PMA conditions, extracted from Figs. 6(a) and 6(b).

rich defects rather than the interaction between H and V_{O} . For devices with IGZO channel, additional FG PMA also induces more positive ΔV_{TH} since the suppression of O-rich defects reduces negative ΔV_{TH} component. Fig. 5(d) summarizes the possible dominant PBTI degradation mechanisms in OS transistors. The dominant negative ΔV_{TH} mechanisms during PBTI stress differ significantly between O-rich and O-poor devices due to different defect types.

FG PMA after O_2 PDA leads to more positive V_{TH} in the transfer characteristics and enhanced PBTI reliability by suppressing O-rich defects. However, a small amount of V_{O} may still exist in O-rich devices and the interaction between H and V_{O} will degrade the device performance. Therefore, PMA under different atmospheres, including N_2 , FG, and VAC, are performed. The effects of PMA under different atmospheres on TG In_2O_3 transistors are shown in Fig. 6(a). PMA under all O-free atmospheres induces a positive ΔV_{TH} , with the magnitude of ΔV_{TH} increasing with PMA temperature, indicating O-rich defects exhibit donor-like behavior and thermal treatment can effectively suppress O-rich defects. Fig. 6(b) compares PBTI performances of TG In_2O_3 transistors under different PMA conditions. All O-free PMA enhance reliability by reducing the magnitude of negative ΔV_{TH} , confirming O-rich defects also induce negative ΔV_{TH} in PBTI performance. Devices with FG PMA exhibit more negative V_{TH} in the transfer characteristics and ΔV_{TH} during PBTI stress compared to devices with VAC PMA or N_2 PMA, suggesting the existence of a small amount of V_{O} even in O-rich films, which will react with H after FG PMA. Figs. 6(c) and 6(d) present μ_{FE} , SS, V_{TH} and $|\Delta V_{\text{TH}}|$ under PBTI measurement at $V_{\text{stress}}=3$ V for 1 ks of the TG In_2O_3 transistors under different PMA conditions. Devices with all O-free PMA show more positive V_{TH} in the transfer characteristics and enhanced reliability. By further eliminating the influence of H, devices with N_2 or VAC PMA demonstrate high μ_{FE} , steep SS, high reliability and relatively positive V_{TH} . The high performance is achieved by O_2 PDA and O-free PMA, which suppress both O-poor and O-rich defects.

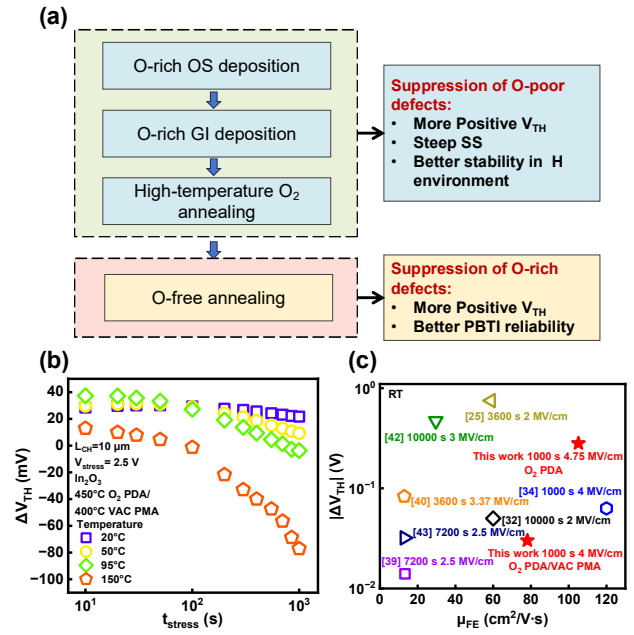


Fig. 7 (a) Strategies for achieving high-mobility and high-stability TG OS transistors. (b) ΔV_{TH} versus t_{stress} characteristics of TG In_2O_3 transistors with O_2 PDA and VAC PMA measured at different temperatures. (c) Benchmark of PBTI reliability at RT versus μ_{FE} of TG OS transistors.

Fig. 7(a) summarizes the effective strategy for enhancing the reliability of high-mobility TG In-rich OS transistors. The O-rich device fabrication process followed by O_2 annealing could suppress O-poor defects, leading to more positive V_{TH} , steep SS, and better stability in H environment. However, O-rich defects will be introduced during the suppression of O-poor defects, resulting in more negative V_{TH} and poor PBTI reliability. Therefore, O-free annealing is needed to suppress O-rich defects, resulting in more positive V_{TH} and better PBTI reliability. The suppression of both O-poor and O-rich defects improve the device performance, overcoming the mobility-stability trade-off. Fig. 7(b) presents PBTI performance of TG In_2O_3 transistors with 450°C O_2 PDA and 400°C VAC PMA measured at different temperatures. The high-mobility In-rich device maintains high reliability even at elevated temperatures, due to both O-poor and O-rich defects are suppressed. Fig. 7(c) benchmarks the PBTI reliability of TG OS transistors measured at RT. By further suppress O-rich defects, the devices demonstrate high μ_{FE} of $78 \text{ cm}^2/\text{V}\cdot\text{s}$ and a low $|\Delta V_{\text{TH}}|$ of 30 mV at RT, V_{stress} of 3 V, and t_{stress} of 1 ks. The TG In_2O_3 transistors with O_2 PDA and O-free PMA in this work exhibit both high reliability and high μ_{FE} , demonstrating the effectiveness of the proposed method, O-rich device fabrication processes followed by O-free annealing, for optimizing the performance of high-mobility TG In-rich OS transistors to overcome the mobility-stability trade-off.

IV. CONCLUSION

In conclusion, we demonstrate TG ALD In-rich OS transistors with high μ_{FE} , steep SS, high reliability and high stability in H environment. The performance enhancement is achieved by O-rich device fabrication processes followed by O-free PMA, resulting in the suppression of both O-poor and O-

rich defects. The distinct difference in defect characteristics and PBTI degradation mechanisms between O-rich and O-poor devices is clarified. The understanding of different defect types provides a new insight to overcome the mobility-stability trade-off.

ACKNOWLEDGMENT

The authors also gratefully acknowledge the support from Huawei corp. for IGZO deposition.

REFERENCES

- [1] Q. Li et al., "BEOL-Compatible High-Performance a-IGZO Transistors with Record high $I_{ds,max} = 1207 \mu A/\mu m$ and on-off ratio exceeding 10^{11} at $V_{ds} = 1V$," in *IEDM Tech. Dig.*, p. 2-7, 2022, doi: 10.1109/IEDM45625.2022.10019448.
- [2] C. Niu et al., "Record-Low Metal to Semiconductor Contact Resistance in Atomic-Layer-Deposited In_2O_3 TFTs Reaching the Quantum Limit," in *IEDM Tech. Dig.*, p. 37-2, 2023, doi: 10.1109/IEDM45741.2023.10413708.
- [3] K. Hikake et al., "A Nanosheet Oxide Semiconductor FET Using ALD InGaOx Channel and InSnOx Electrode with Normally-off Operation, High Mobility and Reliability for 3D Integrated Devices," in *Proc. Symp. VLSI Technol.*, p. T14-1, 2023, doi: 10.23919/VLSITECHNOLOGYANDCIR57934.2023.10185234.
- [4] W. Kim et al., "Demonstration of crystalline IGZO transistor with high thermal stability for memory applications," in *Proc. Symp. VLSI Technol.*, p. T17-4, 2023, doi: 10.23919/VLSITECHNOLOGYANDCIR57934.2023.10185258.
- [5] S. Fujii et al., "Oxide-semiconductor Channel Transistor DRAM (OCTRAM) with $4F^2$ Architecture," in *IEDM Tech. Dig.*, p. 6-1, 2024, doi: 10.1109/IEDM50854.2024.10873368.
- [6] K. H. Chiang et al., "Integration of 0.75 V V_{DD} Oxide-Semiconductor 1T1C Memory with Advanced Logic for An Ultra-Low-Power Low-Latency Cache Solution," in *Proc. Symp. VLSI Technol.*, p. T2-1, 2025, doi: 10.23919/VLSITECHNOLOGYANDCIR65189.2025.11074854.
- [7] T. C. Chiang, Y. C. Chang, C. R. Huang, C. H. Hsu, and P. T. Liu, "First Demonstration of BEOL-Compatible ALD-Deposited 2 nm-Thick Indium-Tungsten-Tin-Oxide (IWTO) TFTs with Superior Short-Channel Electrical Characteristics: Achieving Enhancement-Mode V_{TH} , $I_{ON/OFF} > 10^{10}$, $SS \sim 63.3$ mV/dec," in *Proc. Symp. VLSI Technol.*, p. T12-1, 2025, doi: 10.23919/VLSITECHNOLOGYANDCIR65189.2025.11075200.
- [8] A. Chasin et al., "Understanding and modelling the PBTI reliability of thin-film IGZO transistors," in *IEDM Tech. Dig.*, p. 31-1, 2021, doi: 10.1109/IEDM19574.2021.9720666.
- [9] Y. Magari, T. Kataoka, W. Yeh, and M. Furuta, "High-mobility hydrogenated polycrystalline In_2O_3 ($In_2O_3:H$) thin-film transistors," *Nat. Commun.*, vol. 13, no. 1078, 2022, doi: 10.1038/s41467-022-28480-9.
- [10] Z. Zhang, Z. Lin, C. Niu, M. Si, M. A. Alam, and P. D. Ye, "Ultrahigh Bias Stability of ALD In_2O_3 FETs Enabled by High Temperature O_2 Annealing," in *Proc. Symp. VLSI Technol.*, p. T11-3, 2023, doi: 10.23919/VLSITECHNOLOGYANDCIR57934.2023.10185292.
- [11] M. H. Cho, C. H. Choi, M. J. Kim, J. S. Hur, T. Kim, and J. K. Jeong, "High-Performance Indium-Based Oxide Transistors with Multiple Channels Through Nanolaminate Structure Fabricated by Plasma-Enhanced Atomic Layer Deposition," *ACS Appl. Mater. Interfaces*, vol. 15, no. 15, p. 19137, 2023, doi: 10.1021/acsami.3c00038.
- [12] Q. Jiang, K. Jana, K. Toprasertpong, S. Liu, and H. S. P. Wong, "Positive Bias Stress Measurement Guideline and Band Analysis for Evaluating Instability of Oxide Semiconductor Transistors," in *Proc. Symp. VLSI Technol.*, p. T16-2, 2024, doi: 10.1109/VLSITECHNOLOGYANDCIR46783.2024.10631369.
- [13] A. Chasin et al., "Unraveling BTI in IGZO devices: Impact of device architecture, channel film deposition method and stoichiometry/phase, and device operating conditions," in *IEDM Tech. Dig.*, p. 34-2, 2024, doi: 10.1109/IEDM50854.2024.10873388.
- [14] Z. Lin et al., "First Direct Observation of Two Different Hydrogen-Related Processes Corresponding to the Negative V_{TH} Shift Under PBTI Stress in IGZO Transistors by Pd Hydrogen Spillover," in *Proc. Symp. VLSI Technol.*, p. T17-4, 2025, doi: 10.23919/VLSITECHNOLOGYANDCIR65189.2025.11075056.
- [15] Z. Wang et al., " In_2O_3 -ZnO Superlattice Transistors by Atomic Layer Deposition with High Field-Effect Mobility," *IEEE Electron Device Lett.*, vol. 46, no. 3, p. 412, 2025, doi: 10.1109/LED.2025.3532673.
- [16] Y.-S. Shiah et al., "Mobility-stability trade-off in oxide thin-film transistors," *Nat. Electron.*, vol. 4, p. 800, 2021, doi:10.1038/s41928-021-00671-0.
- [17] Y. Kang et al., "Hydrogen bistability as the origin of photo-bias-thermal instabilities in amorphous oxide semiconductors," *Adv. Electron. Mater.*, vol. 1, no. 7, p. 140006, 2015, doi: 10.1002/aelm.201400006.
- [18] J. Bang, S. Matsuishi, H. Hosono, "Hydrogen anion and subgap states in amorphous In-Ga-Zn-O thin films for TFT applications," *Appl. Phys. Lett.*, vol. 110, no. 23, p. 232105, 2017, doi: 10.1063/1.4985627.
- [19] A. Janotti, and C. G. Van De Walle, "Oxygen vacancies in ZnO," *Appl. Phys. Lett.*, vol. 87, no. 12, p. 122102, 2005, doi: 10.1063/1.2053360.
- [20] A. Janotti, and C. G. Van De Walle, "Hydrogen multicentre bonds," *Nat. Mater.*, vol. 6, P. 44, 2007, doi: 10.1038/nmat1795.
- [21] W. Pan et al., "Multiple effects of hydrogen on InGaZnO thin-film transistor and the hydrogenation-resistivity enhancement," *J. Alloys Compd.*, vol. 947, p. 169509, 2023, doi: 10.1016/j.jallcom.2023.169509.
- [22] Z. Lin et al., "The Role of Oxygen Vacancy and Hydrogen on the PBTI Reliability of ALD IGZO Transistors and Process Optimization," *IEEE Trans. Electron Devices*, vol. 71, no. 5, p. 3002, 2024, doi: 10.1109/TED.2024.3374247.
- [23] G. Liu et al., "Revealing the Impact of Hydrogen (H) on NBTI/PBTI of IGZTO FETs Under DC and AC Stress: Deep Dive into H Dynamics and Advanced Modeling," in *IEDM Tech. Dig.*, p. 34-3, 2024, doi: 10.1109/IEDM50854.2024.10873553.
- [24] M. Si, A. Charnas, Z. Lin, and P. D. Ye, "Enhancement-Mode Atomic-Layer-Deposited In_2O_3 Transistors with Maximum Drain Current of 2.2 A/mm at Drain Voltage of 0.7 V by Low-Temperature Annealing and Stability in Hydrogen Environment," *IEEE Trans. Electron Devices*, vol. 68, no. 3, p.1075, 2021, doi: 10.1109/TED.2021.3053229.
- [25] C. H. Choi et al., "High-Performance Indium Gallium Tin Oxide Transistors with an Al_2O_3 Gate Insulator Deposited by Atomic Layer Deposition at a Low Temperature of 150°C: Roles of Hydrogen and Excess Oxygen in the Al_2O_3 Dielectric Film," *ACS Appl. Mater. Interfaces*, vol. 13, no. 24, p. 28451, 2021, doi: 10.1021/acsaami.1c04210.
- [26] Y.-S. Kim et al., "Remarkable Stability Improvement with a High-Performance PEALD-IZO/IGZO Top-Gate Thin-Film Transistor via Modulating Dual-Channel Effects," *Adv. Mater. Interfaces*, vol. 9, no. 16, p. 2200501, 2022, doi: 10.1002/admi.202200501.
- [27] C. Gu et al., "High-Performance Short-Channel Top-Gate Indium-Tin-Oxide Transistors by Optimized Gate Dielectric," *IEEE Electron Device Lett.*, vol. 44, no. 5, p. 837, 2023, doi: 10.1109/LED.2023.3262684.
- [28] J.-Y. Lin et al., "First Demonstration of Top-Gate Enhancement-Mode ALD In_2O_3 FETs with High Thermal Budget of 600°C for DRAM Applications," *IEEE Electron Device Lett.*, vol. 45, no. 10, p. 1851, 2024, doi: 10.1109/LED.2024.3442729.
- [29] Y. Han et al., "Abnormal Positive Shift of Threshold Voltage in Praseodymium-Doped InZnO-TFTs Under Negative Bias Illumination Temperature Stress," *IEEE Trans. Electron Devices*, vol. 71, no. 3, p. 1951, 2024, doi: 10.1109/TED.2024.3359160.
- [30] S. Wahid et al., "Role of Oxygen Deficiencies on the Stability of Indium Tin Oxide (ITO) Transistors," *IEEE Electron Device Lett.*, vol. 46, no. 9, p. 1553, 2025, doi: 10.1109/LED.2025.3587706.
- [31] J. E. Oh et al., "In-situ Surface Energy Engineering for ALD-Derived Highly Reliable Top Gate In_2O_3 Thin-Film Transistors," *IEEE Electron Device Lett.*, vol. 46, no. 11, p. 2050, 2025, doi: 10.1109/LED.2025.3606470.
- [32] J.-H. Yoo et al., "Process design for improvement in device performance of top-gate TFTs using In-Sn-Zn-O channels prepared by thermal atomic-layer deposition," *Mater. Sci. Semicond. Process.*, vol. 190, p. 109324, 2025, doi: 10.1016/j.mssp.2025.109324.
- [33] M. M. Billah et al., "Multi-Channel, Amorphous Oxide Thin-Film Transistor Exhibiting High Mobility of $67 \text{ cm}^2 \text{ V}^{-1} \text{ s}^{-1}$ and Excellent Stability," *Adv. Electron. Mater.*, vol. 11, no. 8, p. 2400766, 2025, doi: 10.1002/aelm.202400766.
- [34] C.-S. Huang et al., "High Mobility and Robust Top-Gate In_2O_3 Thin Film Transistor by Ozone-Based Treatment," *IEEE J. Electron Devices Soc.*, vol. 13, p. 1112, 2025, doi: 10.1109/JEDS.2025.3627495.
- [35] J. Park et al., "Improved electrical performance and stability of top-gated indium-tin-zinc-oxide thin-film transistors via oxygen plasma treatment," *Semicond. Sci. Technol.*, vol. 40, no. 11, p. 115013, 2025, doi: 10.1088/1361-6641/ae1869.

-
- [36] S.-H. Kim et al., "Reliability Improvement of High Mobility Oxide TFTs Based on Hydrogen-Resistant PEALD Al₂O₃ Gate Insulators Grown with N₂O Plasma," *ACS Appl. Mater. Interfaces*, vol. 17, no. 9, p. 14168, 2025, doi: 10.1021/acsami.4c18561.
- [37] Z. Lin et al., "The Critical Role of Passivation Layer and Semiconductor Interface on the Hydrogen Stability of ALD IGZO Transistors," *IEEE Trans. Electron Devices*, vol. 72, no. 8, p. 4138, 2025, doi: 10.1109/TED.2025.3575400.
- [38] K. Jiang et al., "Top-Gate Atomic-Layer-Deposited Oxide Semiconductor Transistors With Large Memory Window and Non-Ferroelectric HfO₂ Gate Stack," *IEEE Electron Device Lett.*, vol. 46, no. 8, p. 1353, 2025, doi: 10.1109/LED.2025.3581599.
- [39] J. Li et al., "Near-Ideal Top-Gate Controllability of InGaZnO Thin-Film Transistors by Suppressing Interface Defects with an Ultrathin Atomic Layer Deposited Gate Insulator," *ACS Appl. Mater. Interfaces*, vol. 15, no. 6, p. 8666, 2023, doi:10.1021/acsami.2c20176.
- [40] Y. Guan et al., "Ultra-thin top-gate insulator of atomic-layer-deposited HfO_x for amorphous InGaZnO thin-film transistors," *Appl. Surf. Sci.*, vol. 625, no. 157177, 2023, doi:10.1016/j.apsusc.2023.157177.
- [41] J.-E. Yang et al., "A-IGZO FETs with High Current and Remarkable Stability for Vertical Channel Transistor (VCT)/3D DRAM Applications," in *Proc. Symp. VLSI Technol.*, p. T4.5, 2024, doi: 10.1109/VLSITechnologyandCir46783.2024.10631550.
- [42] Y. J. Seo, J. W. Lee, Y. H. Kwon, N. J. Seong, K. J. Choi, and S. M. Yoon, "Synergistic Effects of Deposition Temperatures for Active and Gate Insulator of Top-Gate Thin-Film Transistors Using InGaZnO Channels Prepared by Thermal Atomic-Layer Deposition," *ACS Appl. Electron. Mater.*, vol. 6, no. 10, p. 7563, 2024, doi: 10.1021/acsaelm.4c01380.
- [43] S. Zheng et al., "Enhancement in Performance and Reliability of Fully Transparent a-IGZO Top-Gate Thin-Film Transistors by a Two-Step Annealing Treatment," *Nanomater.*, vol. 15, no. 6, p. 460, 2025, doi:10.3390/nano15060460.
- [44] X. Li et al., "First Demonstration of Atomic-Interlayer-Tuning Driven by First Principles Calculations and Atomic Layer Deposition towards High Thermal Stable BEOL IGZO-FETs with SS=62mV/dec, PBTI < 7mV@ 3MV/cm and 353K," in *Proc. Symp. VLSI Technol.*, p. T17-3, 2025, doi: 10.23919/VLSITechnologyandCir65189.2025.11075061.